

A Numerical Method for Time-Dependent Infiltration from Periodic Trapezoidal Channels with Different Types of Root-Water Uptake

Imam Solekhudin

Abstract—A time-dependent water infiltration problem in homogeneous soil with water absorption is considered. The problem involves infiltration from periodic trapezoidal channels. Four different root distributions are incorporated into the problem. The governing equation of the problem is the Richards equation, which can be studied more conveniently by transforming the equation into a modified Helmholtz equation. The modified Helmholtz equation may be solved numerically using a Dual Reciprocity Boundary Element Method (DRBEM) and a predictor-corrector scheme simultaneously. Numerical results obtained are to give the distribution of matric flux potential (MFP) and suction potential. The results indicate the influence of the distance of points from the channels to reach their steady state values of MFP and suction potential.

Index Terms—dual reciprocity boundary element method, infiltration, root-water uptake, predictor-corrector, modified Helmholtz equation.

I. INTRODUCTION

THE study of water infiltration through homogeneous soil involving single or periodic channels has been considered by a number of researchers. For instance, Batu [3], Gardner [6], Mandal and Waechter [11], Philip [12], and Lobo et al. [9] considered steady infiltration problems. Time dependent infiltration problems have been studied by, for example, Lomen and Warrick [10], Warrick and Lomen [19], and Clements and Lobo [5].

The infiltration problems are governed by Richards equations. To study the problems, like other engineering problems, numerical methods are employed, as analytical methods may only be applied to solve simple problems. There are numerical methods that are used to solve engineering problems. For instance, Finite Difference Method (FDM), Finite Element Method (FEM), and Boundary Element Method (BEM). An FDM is used by Wongsajai et al [20] for solving the general Rosenau-RLW equation. Hollis et al [7] employed an FEM to compare the accuracy of the direct and MDEV inversion algorithms in MR elastography. In this paper, we solve infiltration problems using a DRBEM.

In this current study, we consider time-dependent infiltration problems from periodic trapezoidal channels with water absorption by plant roots. Four different types of root-water uptake are incorporated in the problems. To study the problems, the governing equation of the problems is transformed into a modified Helmholtz equation using a set of transformations, including the Laplace transform. A numerical procedure, DRBEM with a predictor corrector

scheme, is then applied to solve the modified Helmholtz equation numerically to provide numerical values of matric flux potential (MFP) and suction potential.

II. PROBLEM FORMULATION

Study in this paper is a continuation of the study in Solekhudin [16]. Thus, the problem formulation is similar. Referred to a cartesian coordinate $OXYZ$ with OZ positively downward consider a homogeneous soil, Pima Clay Loam (PCL). On the surface of soil, periodic trapezoidal irrigation channels are constructed. The cross-sectional perimeter of the channels is $2L$. The channels are completely filled with water. It is assumed that the channels are sufficiently long, and there is a large number of such channels. Between two channels, a row of crops, with roots of depth Z_m and width $2X_m$, are planted. The distance between two adjacent rows of plants is $2(L+D)$. It is assumed that the geometry of the channels and root zone do not vary in the OY direction and are symmetric about the planes $X = \pm k(L+D)$, for $k = 0, 1, 2, \dots$. Hence, flow directions are two dimensions. The cross section of the geometry of the problem is shown in Figure 1.

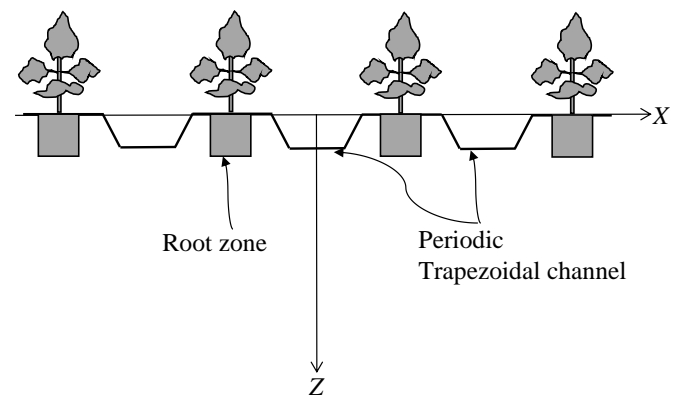


Fig. 1: Periodic trapezoidal channels with crops.

Since the geometry is symmetrical about $X = 0$, it is sufficient to consider a semi infinite region defined by $0 \leq X \leq L+D$ and $Z \geq 0$, which is denoted by R bounded by $C = C_1 \cup C_2 \cup C_3 \cup C_4$ as shown in Figure 2. Fluxes over the surface of channels are assumed to be constant, that is v_0 . On the surface of soil outside the channels, there are no fluxes across it. The fluxes over $X = 0$ and $X = L+D$ are also 0, as the problem symmetric about them. Following Batu in [3], the derivatives $\partial\Theta/\partial X \rightarrow 0$ and $\partial\Theta/\partial Z \rightarrow 0$ as $X^2 + Z^2 \rightarrow \infty$, where Θ is the Matric Flux Potential (MFP).

Manuscript received August 4, 2017; revised December 27, 2017.

I. Solekhudin is with Department of Mathematics, Universitas Gadjah Mada, Yogyakarta, INDONESIA e-mail: (imams@ugm.ac.id).

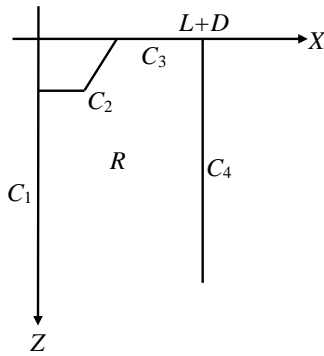


Fig. 2: Region R bounded by curve C .

Four different types of root-water uptake are considered, denoted by Root A, Root B, Root C, and Root D. These types of roots are as reported by Vrugt et al [18]. It is required to determine the matric flux potential and the suction potential. A comparison between the MFP from different types of root-water uptake is presented as well as the suction potentials.

III. BASIC EQUATIONS

Time-dependent infiltration in a homogeneous soil is governed by Richards equation of the form

$$\frac{\partial \theta}{\partial T} = \frac{\partial}{\partial X} \left(K \frac{\partial \psi}{\partial X} \right) + \frac{\partial}{\partial Z} \left(K \frac{\partial \psi}{\partial Z} \right) - \frac{\partial K}{\partial Z} - S(X, Z, \psi), \quad (1)$$

where θ is water content in the soil, T is the time of infiltration, K is the hydraulic conductivity, $\psi(X, Z)$ is the suction potential, and S is the root-water uptake function. Here, S is adopted from the model proposed by Vrugt et al [18], that is

$$S(X, Z, \psi) = \gamma(\psi) \frac{L_t \beta(X, Z) T_{pot}}{\int_0^{Z_m} \int_{L+D-X_m}^{L+D} \beta(X, Z) dX dZ}, \quad (2)$$

where L_t is the width of the soil surface associated with transpiration process, β is the spatial root-water uptake distribution, T_{pot} is the transpiration potential, and γ is the root-water stress response function reported by Utset et al [17]. The spatial root-water uptake, β , is formulated as

$$\beta(X, Z) = \left(1 - \frac{L+D-X}{X_m} \right) \left(1 - \frac{Z}{Z_m} \right) \times e^{-\left(\frac{p_z}{Z_m} |Z^* - Z| + \frac{p_x}{X_m} |X^* - (L+D-X)| \right)},$$

for $L+D-X_m \leq X \leq L+D, 0 \leq Z \leq Z_m$, subject to initial condition

where p_x, p_z, X^* , and Z^* are fitting parameters.

Using the Kirchhoff transformation

$$\Theta = \int_{-\infty}^{\psi} K(t) dt, \quad (3)$$

where Θ is the MFP, and an exponential relationship between K and ψ ,

$$K = K_s e^{\alpha \psi}, \quad (4)$$

where K_s is the saturated hydraulic conductivity, Equation (1) can be written as

$$\frac{\partial \theta}{\partial T} = \frac{\partial^2 \Theta}{\partial X^2} + \frac{\partial^2 \Theta}{\partial Z^2} - \alpha \frac{\partial \Theta}{\partial Z} - S(X, Z, \psi), \quad (5)$$

and the suction potential

$$\psi = \frac{1}{\alpha} \ln \left(\frac{\alpha \Theta}{K_s} \right) \quad (6)$$

Equation (5) can also be written as

$$\frac{1}{D(\theta)} \frac{\partial \Theta}{\partial T} = \frac{\partial^2 \Theta}{\partial X^2} + \frac{\partial^2 \Theta}{\partial Z^2} - \alpha \frac{\partial \Theta}{\partial Z} - S(X, Z, \psi), \quad (7)$$

where $D(\theta)$ is the diffusivity. In field situations, the diffusivity may be assumed as a constant d [2].

Substituting dimensionless variables

$$\begin{aligned} x &= \frac{\alpha}{2} X; & z &= \frac{\alpha}{2} Z; & \Phi &= \frac{\pi \Theta}{v_0 L}; & t &= \frac{\alpha^2 d}{4} T \\ u &= \frac{2\pi}{v_0 \alpha L} U; & v &= \frac{2\pi}{v_0 \alpha L} V; & f &= \frac{2\pi}{v_0 \alpha L} F, \end{aligned} \quad (8)$$

into Equation (7) we obtain

$$\frac{\partial \Phi}{\partial t} = \frac{\partial^2 \Phi}{\partial x^2} + \frac{\partial^2 \Phi}{\partial z^2} - 2 \frac{\partial \Phi}{\partial z} - \gamma^*(\Phi) s^*(x, z), \quad (9)$$

where

$$s^*(x, z) = \frac{2\pi}{\alpha L} \frac{\int_0^{z_m} \int_{b-x_m}^b l_t \beta^*(x, z) dx dz}{\int_0^{z_m} \int_{b-x_m}^b \beta^*(x, z) dx dz} \frac{T_{pot}}{v_0}, \quad (10)$$

$$\gamma^*(\Phi) = \gamma \left(\frac{1}{\alpha} \ln \left(\frac{\alpha v_0 L \Phi}{\pi K_s} \right) \right),$$

and

$$\begin{aligned} \beta^*(x, z) &= \left(1 - \frac{b-x}{x_m} \right) \left(1 - \frac{z}{z_m} \right) \\ &\times e^{-\left(\frac{p_z}{z_m} |z^* - z| + \frac{p_x}{x_m} |x^* - \frac{2(b-x)}{\alpha}| \right)}. \end{aligned} \quad (11)$$

Here $l_t = \frac{\alpha}{2} L_t, x^* = \frac{\alpha}{2} X^*, z^* = \frac{\alpha}{2} Z^*, x_m = \frac{\alpha}{2} X_m, z_m = \frac{\alpha}{2} Z_m, p_x = \frac{\alpha}{2} p_x, p_z = \frac{\alpha}{2} p_z$ and $b = \frac{\alpha}{2} (L+D)$.

Now, the suction potential can be written as

$$\psi = \frac{1}{\alpha} \ln \left(\frac{\alpha v_0 L \Phi}{\pi K_s} \right) \quad (12)$$

To transform Equation (9) into a modified Helmholtz equation, we use the method described in [15], as follows. We first treat the nonlinear term, $\gamma^*(\Phi)$, as a constant.

Making use of Laplace transform

$$\Phi^* = \int_0^{\infty} e^{-st} \Phi dt, \quad (13)$$

$$\Phi(x, z, 0) = 0, \quad (14)$$

into Equation (9) yields

$$s \Phi^* = \frac{\partial^2 \Phi^*}{\partial x^2} + \frac{\partial^2 \Phi^*}{\partial z^2} - 2 \frac{\partial \Phi^*}{\partial z} - \frac{1}{s} \gamma^*(\Phi) s^*(x, z). \quad (15)$$

Applying transformation

$$\Phi^* = \phi e^z, \quad (16)$$

into Equation (15) yields

$$\frac{\partial^2 \phi}{\partial x^2} + \frac{\partial^2 \phi}{\partial z^2} = (1+s)\phi + \frac{1}{s} \gamma^*(\Phi) s^*(x, z). \quad (17)$$

Equation (17) is a modified Helmholtz equation.

Using the set of transformations above, the boundary conditions described in Section II can be written as

$$\frac{\partial \phi}{\partial n} = \frac{2\pi}{\alpha L s} e^{-z} - n_2 \phi, \text{ on the surface of the channel,} \tag{18}$$

$$\frac{\partial \phi}{\partial n} = -\phi, \text{ on the surface of soil outside the channel,} \tag{19}$$

$$\frac{\partial \phi}{\partial n} = 0, \quad x = 0 \text{ and } z \geq 0, \tag{20}$$

$$\frac{\partial \phi}{\partial n} = 0, \quad x = b \text{ and } z \geq 0, \tag{21}$$

$$\frac{\partial \phi}{\partial n} = -\phi, \quad 0 \leq x \leq b \text{ and } z = 0. \tag{22}$$

The term n_2 in Boundary condition (18) is the vertical component of normal vector pointing out region R .

An integral equation for solving Equation (17) is

$$\begin{aligned} \lambda(\xi, \eta)\phi(\xi, \eta, s) = & \iint_R \varphi(x, z; \xi, \eta) \left[(1+s)\phi(x, z, s) \right. \\ & \left. + \frac{1}{s} \gamma^*(\phi) s^*(x, z) e^{-z} \right] dx dz \\ & + \int_C \left[\phi(x, z, s) \frac{\partial}{\partial n} (\varphi(x, z; \xi, \eta)) \right. \\ & \left. - \varphi(x, z; \xi, \eta) \frac{\partial}{\partial n} (\phi(x, z, s)) \right] ds, \end{aligned} \tag{23}$$

where $\varphi(x, z; \xi, \eta) = \frac{1}{4\pi} \ln[(x - \xi)^2 + (y - \eta)^2]$ is the fundamental solution of Laplace equation, and

$$\lambda(\xi, \eta) = \begin{cases} 1/2 & , \text{ for } (\xi, \eta) \text{ on smooth part of } C \\ 1 & , \text{ for } (\xi, \eta) \in R \end{cases}.$$

Equation (23) may be solved using a DRBEM and a predictor-corrector simultaneously. Readers may refer to [14] for the detail of the method.

To compute numerical values of the dimensionless MFP, we first employ Equation (23) to obtain numerical values of ϕ , and then use the Stehfest formula to determine the numerical values of their inverse Laplace transform. The formula is as follows

$$\Phi(x, z, t) \simeq \frac{\log 2}{t} \sum_{n=1}^{2N} K_n \Phi^*(x, z, s_n), \tag{24}$$

where

$$\begin{aligned} s_n &= n \frac{\log 2}{t}, \\ K_n &= (-1)^{(n+N)} \times \\ & \sum_{m=(n+1)/2}^{\min(n,N)} \frac{m^N (2m)!}{(N-m)! m! (m-1)! (n-m)! (2m-n)!} \end{aligned}$$

IV. RESULTS AND DISCUSSION

In this section, some numerical results for steady suction potential associated with infiltration from periodic trapezoidal channels with root-water uptake in Pima Clay Loam (PCL) are presented. The values of α and K_s of PCL are 0.014 cm^{-1} and 9.9 cm/day , respectively [1], [4]. The values of L and D are set to be the same, $L = D = 50 \text{ cm}$. The

width and the depth of the channels are $4L/\pi$ and $3L/2\pi$, respectively. The potential transpiration rate is that used by Li et al [8] and Šimunek and Hopmans [13], that is 4 mm/day .

Four different types of root-water uptake models are considered, namely Root A, Root B, Root C, and Root D. Parameters of the root-water uptake models are summarized in Table I.

TABLE I: Parameter values for four different root-water uptake.

Root type	fitting parameters					
	Z_m	X_m	Z^*	X^*	p_Z	p_X
Root A	100 cm	50 cm	0 cm	0 cm	1.0	1.0
Root B	100 cm	50 cm	20 cm	0 cm	1.0	1.0
Root C	100 cm	50 cm	0 cm	25 cm	1.0	4.0
Root D	100 cm	50 cm	20 cm	25 cm	5.0	2.0

To employ the DRBEM, the domain of the problem must be bounded by a simple closed curve. An appropriate value of z for boundary conditions to be applied without significant impact to values of ϕ in the domain is $z = 4$. Therefore, the domain is set to be between $z = 0$ and $z = 4$. The boundary is divided into 404 constant elements, and 892 interior points are chosen.

After obtaining numerical values of ϕ , values of Φ^* can be computed using Equation (16). Finally, employing the Stehfest formula (24) with $N = 3$, dimensionless MFP, Φ , are obtained. Some of the results are presented in Tables II - VII, and Figures 3 and 4.

TABLE II: Values of dimensionless MFP, Φ , at (0.1,0.5).

t	Root A	Root B	Root C	Root D
0.8	2.02857736	2.02972843	2.02539080	2.02145953
1.0	2.13827636	2.13943751	2.13412796	2.13017752
2.0	2.34567542	2.34700183	2.34081485	2.33652156
3.0	2.39097238	2.39233939	2.38595902	2.38161918
4.0	2.40365782	2.40503665	2.39859328	2.39424435
5.0	2.40753647	2.40891926	2.40245327	2.39810319

TABLE III: Values of dimensionless MFP, Φ , at (0.1,2.0).

t	Root A	Root B	Root C	Root D
0.8	0.85211076	0.85287730	0.84096029	0.84431240
1.0	1.13074747	1.13158442	1.11559336	1.11920974
2.0	1.86576136	1.86725319	1.84641029	1.84928421
3.0	2.09026653	2.09196709	2.06985183	2.07249748
4.0	2.16574491	2.16751736	2.14497224	2.14754514
5.0	2.19319539	2.19499652	2.17229139	2.17483733

TABLE IV: Values of dimensionless MFP, Φ , at (0.35,0.5).

t	Root A	Root B	Root C	Root D
0.8	1.79871882	1.79955480	1.79507132	1.79065268
1.0	1.90946308	1.91042604	1.90514156	1.90064892
2.0	2.11841794	2.11959560	2.11346024	2.10863147
3.0	2.16397572	2.16519995	2.15886639	2.15398627
4.0	2.17672192	2.17795978	2.17156180	2.16667113
5.0	2.18061496	2.18185745	2.17543629	2.17054406

TABLE V: Values of dimensionless MFP, Φ , at (0.35,2.0).

t	Root A	Root B	Root C	Root D
0.8	0.85069505	0.85114437	0.83922682	0.84234599
1.0	1.12931030	1.13004565	1.11448494	1.11780797
2.0	1.86431033	1.86575390	1.84545244	1.84805360
3.0	2.08881798	2.09047426	2.06889600	2.07127276
4.0	2.16429758	2.16602621	2.14401724	2.14632094
5.0	2.19174845	2.19350527	2.17133622	2.17361356

TABLE VI: Values of dimensionless MFP, Φ , at (0.5,0.5).

t	Root A	Root B	Root C	Root D
0.8	1.65297969	1.65369249	1.64974500	1.64552561
1.0	1.76438716	1.76512293	1.76014343	1.75578644
2.0	1.97442812	1.97537693	1.96944241	1.96466413
3.0	2.02017404	2.02117525	2.01503188	2.01018334
4.0	2.03296559	2.03398211	2.02777166	2.02290741
5.0	2.03686987	2.03789177	2.03165721	2.02678981

TABLE VII: Values of dimensionless MFP, Φ , at (0.5,2.0).

t	Root A	Root B	Root C	Root D
0.8	0.85018689	0.85067262	0.83869871	0.84188164
1.0	1.12881720	1.12952621	1.11377464	1.11719860
2.0	1.86383430	1.86523616	1.84471214	1.84739942
3.0	2.08834271	2.08995780	2.06815718	2.07061906
4.0	2.16382246	2.16550980	2.14327893	2.14566747
5.0	2.19127341	2.19298901	2.17059806	2.17296024

Tables II-VII show numerical values of the dimensionless MFP, Φ , for various values of t at selected points in the soil with four different root-water uptake models. Specifically, Tables II and III show values of Φ at (0.1, 0.5) and (0.1, 2.0) respectively. Values of Φ at (0.35, 0.5) and (0.35, 2.0) are

shown in Tables IV and V respectively. For points (0.5, 0.5) and (0.5, 2.0), values of Φ at these two points are shown in Tables VI and VII. From Table II and Table III, it can be seen that the infiltration problem with Root B results in the highest values of Φ . On the other hand, Root D results in the lowest values of Φ . It is observed in all cases that the percentages of increase in Φ from a time level to another time level are about the same. From $t = 0.8$ to $t = 1.0$, values of Φ at (0.1, 0.5) and (0.1, 2.0) increase about 5.4% and 32.7% respectively. Increase in values of Φ at these two points are about 9.7% and 65%, from $t = 1$ to $t = 2$, about 1.9% and 12% from $t = 2$ to $t = 3$, about 0.5% and 3.6% from $t = 3$ to $t = 4$, and about 0.2% and 1.3% from $t = 4$ to $t = 5$. These results indicate that percentages of the increase in Φ at deeper position are higher than those at lower position. The results also indicate percentages of the increase in Φ at the beginning of infiltration are higher than those at other times of infiltration.

Table IV and Table V show values of Φ at (0.35, 0.5) and (0.35, 2.0). It can be seen that the results have the same fashion as the results in Table II and Table III. From $t = 0.8$ to $t = 1.0$, values of Φ at these two points increase about 6.2% and 32.8% respectively. Percentage increase in values of Φ at these two points are about 10.9% and 65.1%, from $t = 1$ to $t = 2$, about 2.2% and 12% from $t = 2$ to $t = 3$, about 0.6% and 3.6% from $t = 3$ to $t = 4$, and about 0.2% and 1.3% from $t = 4$ to $t = 5$.

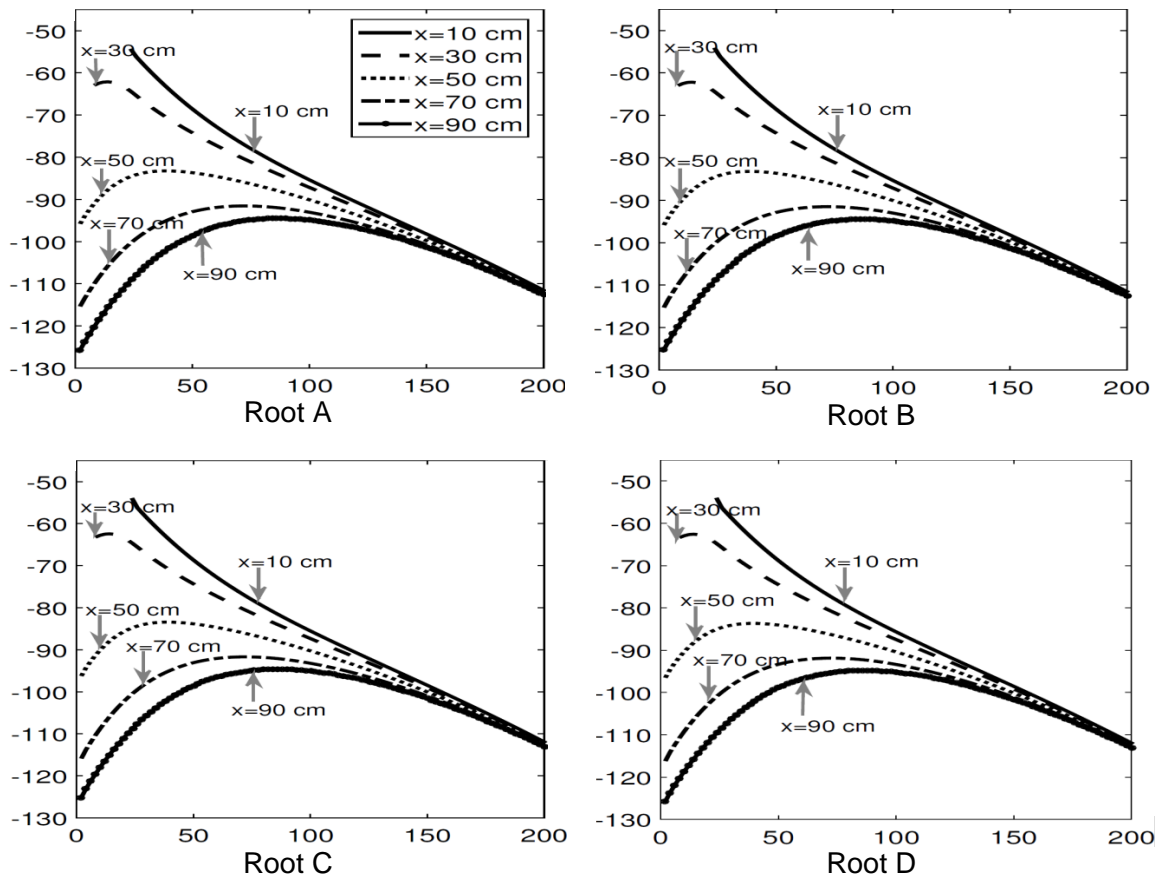


Fig. 3: Values of ψ at different values of X at $t = 0.8$ along Z -axis.

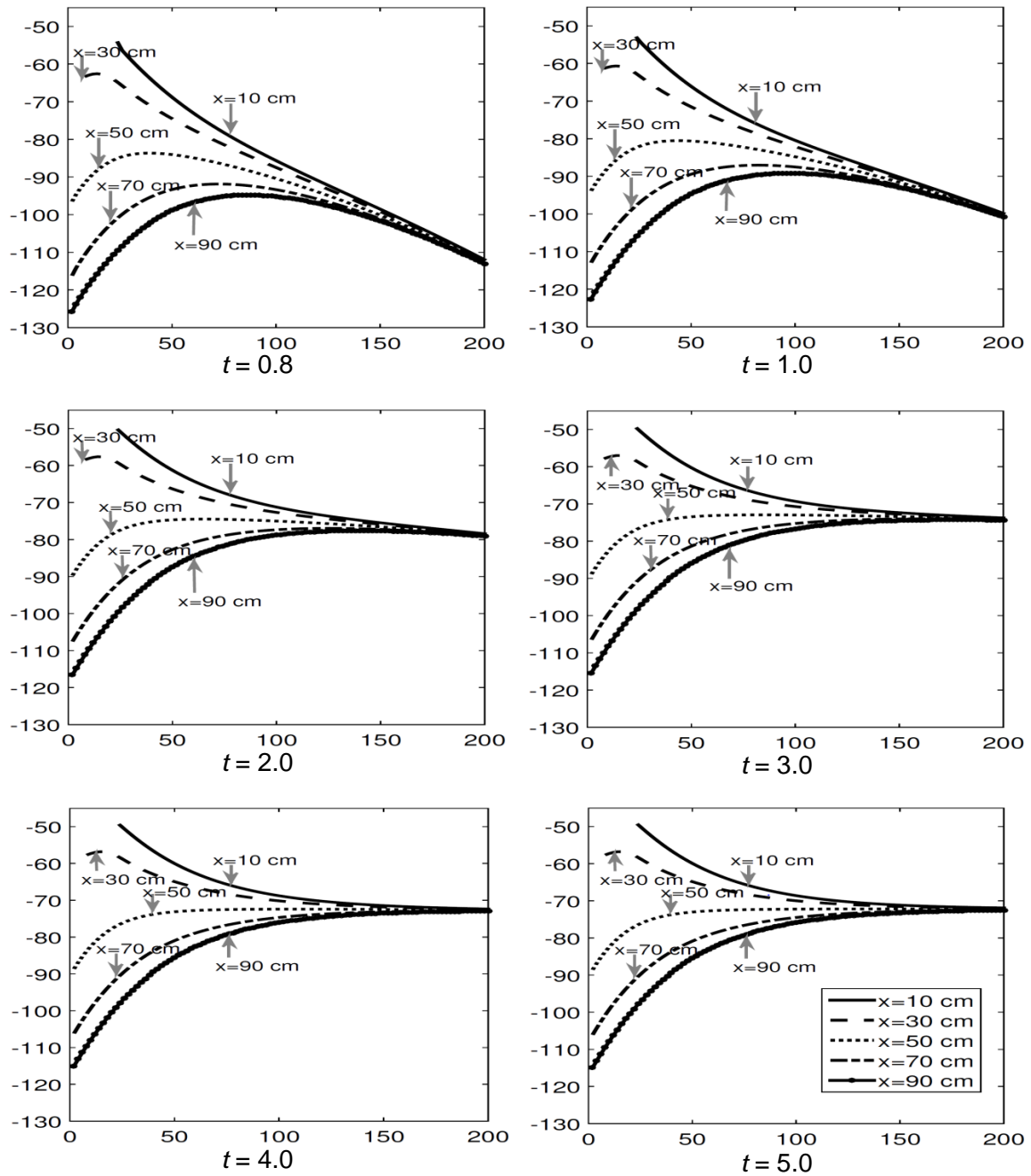


Fig. 4: Values of ψ at different values of X at various time t along Z -axis for infiltration with Root D.

Values of Φ at (0.5, 0.5) and (0.5, 2.0) are shown in Table VI and Table VII, respectively. As before, Root B results in the highest values of Φ , and Root D results in the lowest values of Φ . From $t = 0.8$ to $t = 1.0$, values of Φ at these two points increase about 6.7% and 32.8% respectively. Values of Φ at these two points increase about 11.9% and 65.1%, from $t = 1$ to $t = 2$, about 2.3% and 12.1% from $t = 2$ to $t = 3$, about 0.6% and 3.6% from $t = 3$ to $t = 4$, and about 0.2% and 1.3% from $t = 4$ to $t = 5$. The results presented above indicate that percentages of the increase of Φ at deeper locations are higher than those at shallower. Moreover, the percentage of increase in Φ at points near the channels is lower than those further.

Figure 3 shows values of ψ from infiltration with four different types of root-water uptake at $t = 0.8$ along Z -axis. There are five different values of X . The values of X are 10

cm, 30 cm, 50 cm, 70 cm, and 90 cm. It can be seen from the figure that values of ψ at positions nearer the channels is higher than those further. This result indicates that soils close to the channels more moist than those away. However, for any depth level of soil of c cm, where $c > 150$, the moisture contents at the horizontal level of $z = c$ are about the same.

Figure 3 also shows that there are almost no distinguishes between the four graph. This means that the differences in the values of ψ are relatively small. Hence, to show the values of ψ at different times t , only results from infiltration with Root D are presented in Figure 4.

Figure 4 contains a series of graphs that show the values of ψ , for several different time levels, that is $t = 0.8, 1.0, 2.0, 3.0, 4.0$ and 5.0 , at various values of X along Z -axis. The graphs illustrate the change in the values of ψ as the dimensionless time t increased. From $t = 0.8$ to $t = 1.0$, it

can be seen clearly that the value of ψ increases along Z -axis. This also occur from $t = 1$ to $t = 2$. It is observed that the increase in ψ at deeper level of soil is more significant than those shallower. These mean that there may significant increase in water content in the soil from $t = 0.8$ to $t = 1.0$, as well as from $t = 1.0$ to $t = 2.0$, especially at deeper level of soil.

From $t = 2$ to $t = 3$, it seems that there are no significant increase in the distribution of ψ at the surface of the channel, but at other locations, significant changes are observed. After $t = 3$, the distribution of ψ remains more or less constant over the region. These observations indicate that points at shallower level achieve maximum water content earlier than those deeper. These results obtained are physically meaningful, as irrigation water passes through a shallower level of soil first, before going deeper. At the shallower level, some of the water is absorbed, and then the rest moves through to deeper levels.

The results show that water content in soil increases over time until they reach their maximum levels. The results also indicate that at any given point in time, the amount of water absorbed by the soil at a fixed depth may be the same in all horizontal direction, provided sufficient time is given for infiltration. The results also show that a point at a shallow level of soil depth reaches its maximum water content more rapidly than those at deeper levels.

V. CONCLUDING REMARK

A problem involving time-dependent infiltration from periodic trapezoidal channels with four different types of root uptake has been solved by applying a set of transformations involving Laplace transform and a DRBEM with a predictor-corrector scheme. The method is applied to obtain numerical values of dimensionless MFP and suction potential.

The results obtained indicate that increase in the dimensionless MFP is not affected by the types of root uptake. The results also indicate the variation in time needed to approach the steady state value of the dimensionless MFP and suction potential at different points below the trapezoidal channels. Points at a level need more time than that at shallower levels, which means that points at shallower levels of soil depth reach their maximum water contents faster than those deeper.

REFERENCES

- [1] A. Amoozegar-Fard, A. W. Warrick and D. O. Lomen, "Design Nomographs for Trickle Irrigation System," *J. of Irrigation and Drainage Engineering*, vol. 110, pp. 107 - 120, 1984.
- [2] H. A. Basha, "Multidimensional linearized nonsteady infiltration with prescribed boundary conditions at the soil surface," *Water Resour. Res.* vol. 35, pp. 75 - 83, 1999.
- [3] V. Batu, "Steady Infiltration from Single and Periodic Strip Sources," *Soil Sci. Soc. Am. J.*, vol. 42, pp. 544 - 549, 1978.
- [4] E. Bresler, "Analysis of Trickle Irrigation with Application to Design Problems," *Irrigation Science*, vol. 1, pp. 3 - 17, 1978.
- [5] D. L. Clements and M. Lobo, "A BEM for Time Dependent Infiltration from An Irrigation Channel," *Engineering Analysis with Boundary Elements*, vol. 34, pp. 1100 - 1104, 2010.
- [6] W. R. Gardner, "Some Steady State Solutions of the Unsaturated Moisture Flow Equation with Application to Evaporation from a Water Table," *Soil Sci.*, vol. 85, pp. 228 - 232, 1957.
- [7] L. Hollis, E. Barnhill, N. Conlisk, L. E. J. Thomas-Seale, N. Roberts, P. Pankaj and P. R. Hoskins, "Finite Element Analysis to Compare the Accuracy of the Direct and MDEV Inversion Algorithms in MR Elastography," *IAENG International Journal of Computer Science*, vol. 43(2), pp. 137 - 146, 2016.
- [8] K. Y. Li, R. De Jong and J. B. Boisvert, "An Exponential Root-Water-Uptake Model with Water Stress Compensation," *J. of Hydrol.*, vol. 252, pp. 189 - 204, 2001.
- [9] M. Lobo, D. L. Clements and N. Widana, "Infiltration from irrigation channels in a soil with impermeable inclusions," *ANZIAM J.*, vol. 46, pp. C1055 - C1068, 2005.
- [10] D. O. Lomen and A. W. Warrick, "Time Dependent Linearized Infiltration. II. Line Sources," *Soil Science Society of America Proceedings*, vol. 38, pp. 568 - 572, 1974.
- [11] A. C. Mandal and R. T. Waechter, "Steady Infiltration in Unsaturated Soil from a Buried Circular Cylinder: The Separate Contributions from Top and Bottom Halves," *Water Resour. Res.*, vol. 30, pp. 107 - 115, 1994.
- [12] J. R. Philip, "Steady Infiltration from Buried Point Sources and Spherical Cavities," *Water Resour. Res.*, vol. 4, pp. 1039 - 1047, 1968.
- [13] J. Šimunek and J. W. Hopmans, "Modeling Compensated Root Water and Nutrient Uptake," *Ecol. Model.*, vol. 220, pp. 505 - 521, 2009.
- [14] I. Solekhdin and K. C. Ang, "A DRBEM with a predictor-corrector scheme for steady infiltration from periodic channels with root-water uptake," *Engineering Analysis with Boundary Elements*, vol. 36, pp. 1199 - 1204, 2012.
- [15] I. Solekhdin and K. C. Ang, "A Laplace transform DRBEM with a Predictor-Corrector Scheme for Time-Dependent Infiltration from Periodic Channels with Root-Water Uptake," *Engineering Analysis with Boundary Elements*, vol. 50, pp. 141 - 147, 2015.
- [16] I. Solekhdin, "Water Infiltration from Periodic Trapezoidal Channels with Different Types of Root-Water Uptake," *Far East Journal of Mathematical Sciences*, vol. 100, pp. 2029 - 2040, 2016.
- [17] A. Utset, M. E. Ruiz, J. Garcia and R. A. Feddes, "A SWACROP-based potato root water-uptake function as determined under tropical conditions," *Potato Res.*, vol. 43, pp. 19 - 29, 2000.
- [18] J. A. Vrugt, J. W. Hopmans and J. Šimunek, "Calibration of a Two-Dimensional Root Water Uptake Model," *Soil Sci. Soc. Am. J.* vol. 65, pp. 1027 - 1037, 2001.
- [19] A. W. Warrick and D. O. Lomen, "Time-Dependent Linearized Infiltration: III. Strip and Disk Sources," *Soil Sci. Soc. Am. J.* vol. 40, pp. 639 - 643, 1976.
- [20] B. Wongsajjai, K. Poochinapan and T. Disyadej, "A Compact Finite Difference Method for Solving the General Rosenau-RLW Equation," *IAENG International Journal of Applied Mathematics*, vol. 44(4), pp. 192 - 199, 2014.